2017 American Control Conference
Sheraton Seattle Hotel
May 24–26, 2017, Seattle, USA

# Anti-Delay Closed-Loop Input Shaper to Improve Manual Control of Flexible System

Kittipong Yaovaja, Withit Chatlatanagulchai, and Pisai Yaemprasuan

*Abstract*— **One example of the manual control of flexible system is the crane operator trying to move a swinging payload from point to point as fast and as accurate as possible. The payload swing definitely slows the task. Recent work has proposed placing an input shaper inside the feedback loop, so-called closed-loop signal shaping, to suppress the residual vibration of the flexible system. The residual vibration was successfully suppressed. However, there was a delay between the time the operator stops giving the command and the time the system actually stops. This is due to the modification of the command by placing the input shaper inside the feedback loop. The delay results in lower accuracy in placing the payload because the operator must guess where the system will stop. This paper presents an improvement on the present closed-loop signal shaping by placing the Smith predictor inside the feedback loop. The predictor significantly reduces the delay. Experiments have shown that operators can maneuver the flexible system using less time and with less subjective difficulty.**

## I. Introduction

Input shaping technique was originated by [1] and was later made more robust to uncertainty in mode parameters by [2]. The technique can suppress residual vibration, occurring at the end of move of flexible system, by using the principle of destructive interference of the impulse responses.

Human control of flexible systems, such as crane operator controlling the swinging payload, can be slow, inaccurate, and prone to accidental collision due to the residual vibration. The human control can be benefited from placing the input shaper in front of the flexible plant to shape the command given by the operator so that the shaped command will not excite the residual vibration.

Ref. [3] studied the so-called *closed-loop signal shaping (CLSS)* in which the input shaper is placed inside the loop between the controller and the plant. They pointed out several advantages, besides residual vibration suppression, including easy handling of the hard nonlinearities, eliminating vibration induced by disturbance, and suitability for manual control. Recent applications of CLSS were given in [4], where a bridge crane with distributed-mass payload was controlled by human operator under windy conditions, in [5], where a 3D crane was controlled by a PID controller and CLSS, and in [6], where a helicopter testbed carrying suspended load was controlled by human using CLSS.

Ref. [7] analyzed the stability property of CLSS using root locus and pointed out that CLSS requires quite an accurate plant model to avoid unexpected instability. Ref. [8] studied the effects of closed-loop signal shaping on disturbance and noise rejections and hard nonlinearities.

For automatic control application, it was pointed out by [9] that the time delay brought to the system by placing the input shaper inside the loop can affect the performance of the controller by limiting the bandwidth of the closed-loop system.

When the controller is human, as in manual control, placing the input shaper inside the loop delays the command given by the operator. As a result, the flexible system will not stop at a point when the human operator stops giving the command. The operator must anticipate where the system will stop, which requires experience and mostly results in inaccuracy from overshooting, human stress due to subjective difficulty, and long time to complete the task.

Several techniques, aimed to reduce the overshoot, have been proposed in the literature. In [10] and [11], a so-called *reduced-modification (RM) input shaper* was presented to maintain the similarity between the operator command, $u$, and the plant control input, $f$. In order to imitate the operator command, $u$, the resulting input shaper has a larger initial impulse, followed by smaller impulses to cancel vibration. In [12], a similar modification was performed to the unity-magnitude (UM) shaper so that human operator perceives less of an input-shaping lag, so-called *reduced-perceived-lag (RPL) shaper*. However, their robustness to modeling errors becomes increasingly poor and their time duration becomes increasingly long.

Ref. [13] presented a so-called *reduced overtravel (RO)* and *zero overtravel (ZO)* input shapers. The RO shaper was designed to limit the shaper-induced overtravel to zero, whereas the ZO shaper was designed to remove the remaining overtravel from unshaped reference due to acceleration limits. However, both shapers contain negative impulses and therefore may cause overcurrenting or excite high modes. Ref. [14] proposed using a predictive element in the graphical user interface so that the operator can see where the crane will stop in advance as a result of overtravel.

K. Yaovaja is with the Department of Mechanical Engineering, Faculty of Engineering at Sriracha, Kasetsart University Sriracha Campus, Chonburi 20230, Thailand.

W. Chatlatanagulchai was with Purdue University, USA. He is now an associate professor of the Department of Mechanical Engineering, Kasetsart University, Bangkok 10900, Thailand (phone: 662-942-8555; fax: 662-579-4576; e-mail: fengwtc@ku.ac.th).

P. Yaemprasuan is with the Control of Robot and Vibration Laboratory, Department of Mechanical Engineering, Kasetsart University, Bangkok 10900 Thailand.

Ref. [15] and [16] shortened the original command by the length of the input shaper so that the shaped command will have the same length as the original command, a so-called *equal-length input shaper*. However, to still obtain the same desired final position, the shortened original command will have higher amplitudes than the original command, requiring the system to have additional unused control authority.

This paper proposed a novel technique to handle the overshoot due to the time delay by incorporating the Smith predictor inside the loop to remove the effect of time delay from the loop.

Advantages of the proposed technique over existing techniques are

- The operator will not feel the delay because the delay is moved out of the loop. This leads to more accuracy, shorter time, and less difficulty to complete the task.
- No modification is required on the input shaper.

This paper is organized in the following order. Section 2 contains the closed-loop signal shaping and an experiment on a two-mass flexible plant showing the overshoot problem. Section 3 discusses the proposed anti-delay closed-loop input shaping with the same experiment without the overshoot. Section 4 presents application of the technique to a 3D crane together with experimental result. Conclusions are in Section 5.

## II. Closed-Loop Signal Shaping

Closed-loop signal shaping (CLSS) was presented in [3]. Its diagram is shown in Fig. 1, where $P$ is the flexible plant, $IS$ is the input shaper, $C$ represents a primary controller, $NL$ represents the hard nonlinearities, $r$ is the reference signal, $u$ is the control effort, $d_I$ is the plant-input disturbance, $d_O$ is the plant-output disturbance, $n$ is the noise, and $y$ is the output of interest.

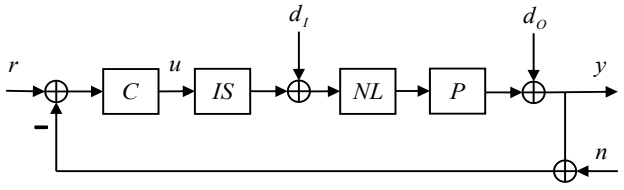


Fig. 1 Closed-loop signal shaping.

Advantages of CLSS, as discussed in [8], are the ability to suppress vibrations induced by $r, d_O,$ and $n$; the ease in handling the hard nonlinearities such as saturation, deadzone, or backlash; and the applicability of manual control when the controller, $C$, is a human operator. However, the CLSS cannot suppress vibration induced by $d_I$, and the CLSS requires accurate plant model to avoid unexpected instability. Another important disadvantage, as pointed out in [9], is that the time-delay terms, brought about by placing the input shaper inside the loop, limit the control bandwidth. Conventional control design and analysis also do not apply since the time-delay term, $e^{-ts}$, is a transcendental function of $s$.

Manual control of flexible systems using CLSS was recently studied in [17]-[11]. The time-delay terms, brought about by the input shaper, modify the command from the human operator. From Fig. 1, the command, $u$, from the human operator, $C$, is modified by the input shaper, $IS$, before going into the plant, $P$. As a result, the plant will not response as the operator intends.

To clearly show this disadvantage, consider an example of a two-mass flexible system, shown in Fig. 2. The mass, $m_1$, represents the rigid-body mass whereas the mass, $m_2$, represents the flexible-body mass. $x_1$ and $x_2$ are the absolute positions of $m_1$ and $m_2$, respectively. $c_1$ and $c_2$ are damping constants of the rigid and flexible parts. $k_2$ is the spring constant, representing the flexibility. $f$ is the force, acting on the rigid-body mass.

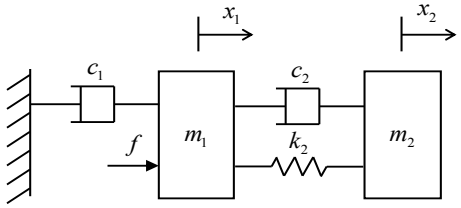


Fig. 2 Two-mass flexible system.

Fig. 3 shows the block diagram of the manual control of the two-mass flexible system, using the closed-loop signal shaping. $C$ is the human operator. The objective is to command the masses, $m_1$ and $m_2$, from point to point, as quickly as possible with the least residual vibration. The human operator does so by observing the rigid-body position, $x_1$, as feedback and trying to make it track the reference. The flexible-body position, $x_2$, should have the little vibration because of the input shaper. However, it will be seen that because the input shaper modifies the operator's original command, $u$, to the time-delayed force, $f$, it is difficult for the operator to control the rigid-body position.

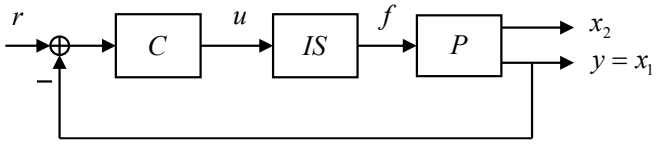


Fig. 3 Closed-loop signal shaping for the two-mass flexible system.

The state equation of the plant, $P$, is given by

$$\begin{bmatrix} \dot{x}_1 \\ \ddot{x}_1 \\ \dot{x}_2 \\ \ddot{x}_2 \end{bmatrix} = \begin{bmatrix} 0 & 1 & 0 & 0 \\ \frac{-k_2}{m_1} & \frac{-(c_1+c_2)}{m_1} & \frac{k_2}{m_1} & \frac{c_2}{m_1} \\ 0 & 0 & 0 & 1 \\ \frac{k_2}{m_2} & \frac{c_2}{m_2} & \frac{-k_2}{m_2} & \frac{-c_2}{m_2} \end{bmatrix} \begin{bmatrix} x_1 \\ \dot{x}_1 \\ x_2 \\ \dot{x}_2 \end{bmatrix} + \begin{bmatrix} 0 \\ 1/m_1 \\ 0 \\ 0 \end{bmatrix} f.$$

For simulation, let $c_1 = 50$ kg/s, $c_2 = 0.1$ kg/s, $m_1 = 10$ kg, $m_2 = 1$ kg, and $k_2 = 10$ kg/s$^2$. The plant, $P$, has a natural frequency of $\omega_n = 3.21$ rad/s and a damping ratio of $\zeta = 0.039$. For simplicity, the ZV input shaper was used in the simulation. Its impulse amplitudes and time locations

were computed as

$$\begin{bmatrix} A_i \\ t_i \end{bmatrix} = \begin{bmatrix} 0.53 & 0.47 \\ 0 & 0.98 \end{bmatrix}.$$

$C$ is a human operator that gives a command, $u$, to the system via a joystick. The operator observes the rigid-body position, $x_1$, and tries to make it track the reference, $r$. Using the closed-loop signal shaping in Fig. 3, typical manual control result is shown in Fig. 4. In Fig. 4(a), the dotted line is the reference, $r$, and the solid line is the rigid-body position, $y = x_1$. In Fig. 4(b), the dotted line is the command, $u$, given by the operator, and the solid line is the shaped command, $f$, given to the plant.

In Fig. 4, "A" marks the time when the operator stops giving the command, $u$, because he/she sees that the rigid-body position, $x_1$, is already at the reference, $r$. However, because the input shaper changes the command, $u$, to the plant control input, $f$, which contains a time-delayed step, the rigid-body position, $x_1$, overshoots its reference, $r$.

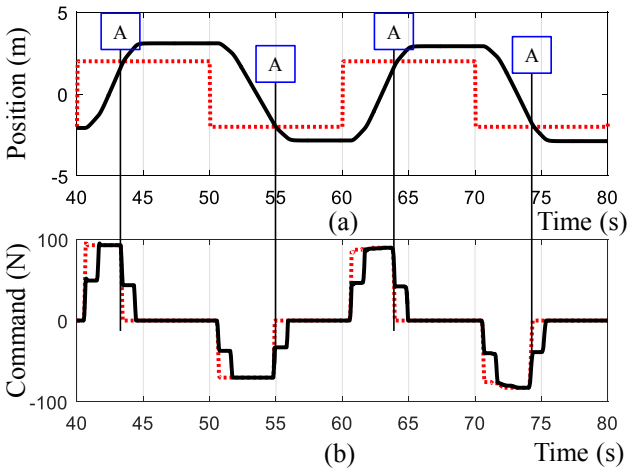


Fig. 4 Manual control result using closed-loop signal shaping. (a) Reference $r$ (dotted line) versus rigid-body position $y$ (solid line). (b) Operator command $u$ (dotted line) versus plant control input $f$ (solid line).

In practice, to avoid the overshoot, the operator must anticipate the stop position of the rigid body and must stop giving the command, $u$, before the rigid body reaches the reference. This results in poor accuracy and control difficulty for the human operator.

## III. Anti-Delay Closed-Loop Input Shaping

Anti-delay closed-loop input shaping (Anti-delay CLIS) was proposed in [9] and [19]. Its diagram for the two-mass flexible system is shown in Fig. 5. *SM* represents the classical Smith predictor, whose transfer function is

$$SM(s) = \hat{P}(s) - \hat{P}(s)IS(s), \tag{1}$$

where $\hat{P}$ is the mathematical model of the actual plant, $P$. $v$ is the output from the Smith predictor. From (1), it can be seen that $v$ contains a prediction of $y$ delayed-time units into the future, hence the name *predictor*.

For the perfect plant model case, when $\hat{P} = P$, the closed-loop transfer function from $r$ to $y$ can be computed as

$$\frac{y(s)}{r(s)} = \frac{C(s)IS(s)P(s)}{1 + C(s)P(s)}. \tag{2}$$

It can be seen that the input shaper, $IS(s)$, no longer appears in the denominator of the closed-loop transfer function. Therefore, the input shaper no longer affects the operator command, $u$. In fact, the transfer function (2) is comparable to the diagram shown in Fig. 6, where the effect of the input shaper, *IS*, is completely moved outside the loop.

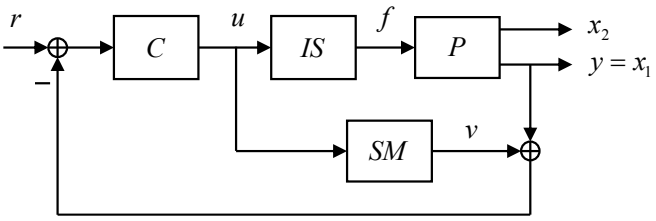


Fig. 5 Anti-delay closed-loop input shaping for the two-mass flexible system.

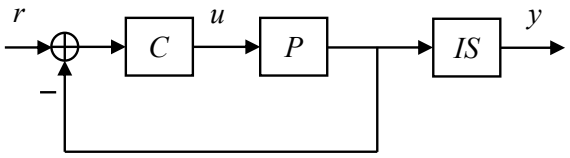


Fig. 6 Comparable block diagram of the anti-delay closed-loop input shaping.

The proposed anti-delay CLIS in Fig. 5 was applied to the manual control of the previous two-mass flexible system with perfect plant model. Fig. 7 contains typical manual control result. In Fig. 7(a), the dotted line is the reference, $r$, the dashed-dotted line is the rigid-body position, $y = x_1$, the solid line is the feedback signal, $v + y$, and the dashed line is the predictor output, $v$. In Fig. 7(b), the dotted line is the operator command, $u$, and the solid line is the control input, $f$, to the plant.

In Fig. 7, "B" marks the time when the operator stops giving the command, $u$, because he/she sees that the feedback signal, $v + y$, is already at the reference, $r$. Because the rigid-body position, $y$, follows the feedback signal by the delayed time of the input shaper, the time-delayed step in the plant control input, $f$, drives the rigid-body position to the reference without overshoot. This results in increasing tracking performance and decreasing subjective difficulty for the human operator, as will be seen in the subsequent sections.

When the plant model is not perfect, that is, when $\hat{P} \neq P$, the closed-loop transfer function then becomes

$$\frac{y(s)}{r(s)} = \frac{C(s)IS(s)P(s)}{1 + C(s)\hat{P}(s) - C(s)\hat{P}(s)IS(s) + C(s)IS(s)P(s)}.$$

The effect of the input shaper, *IS*, is not removed in its totality from the denominator of the closed-loop transfer function and still affects the control system. Then, the performance of the anti-delay CLIS depends on how close the plant model is to

the actual plant. This issue of robustness will be further investigated experimentally in the subsequent sections.

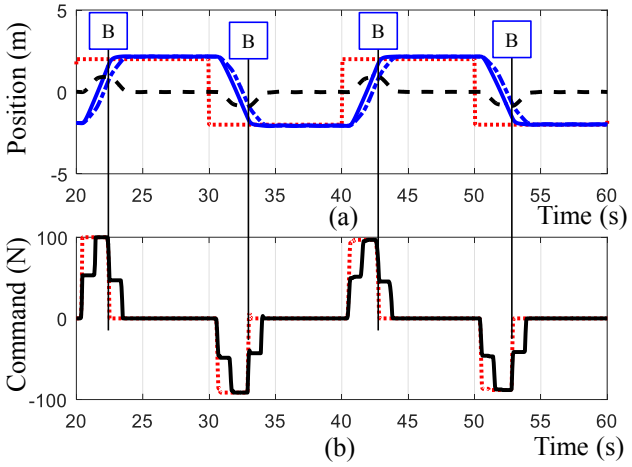


Fig. 7 Manual control result using anti-delay CLIS. (a) Reference $r$ (dotted line), rigid-body position $y$ (dashed-dotted line), feedback signal $v + y$ (solid line), and predictor output $v$ (dashed line). (b) Operator command $u$ (dotted line) versus plant control input $f$ (solid line).

## IV. 3D Crane

The proposed anti-delay CLIS was applied to the manual control of a 3D crane, whose diagram is shown in Fig. 8. $xyz$ is the fixed coordinate frame of the crane. $l$ is the rope length from the cart to the payload. $\theta_x$ and $\theta_y$ are the rope angles to the $yz$ and $xz$ planes, respectively. The human operator uses the joystick to command the cart to move the payload to the target. The cart position is marked by the circle; the payload position is marked by the triangle; and the target position is marked by the square. Because the payload oscillates, it normally is a slow and difficult task for the human operator.

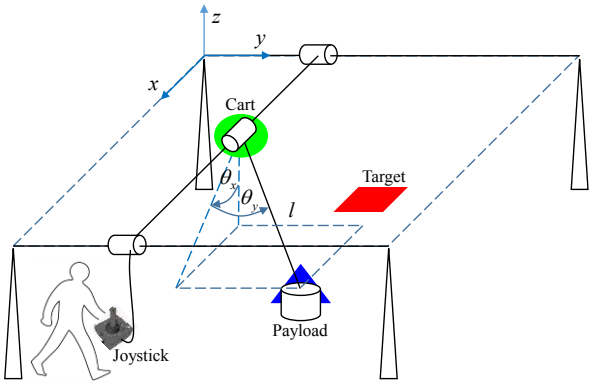


Fig. 8 Diagram of a 3D crane with manual control via a joystick.

Several real human operators were participated in the experiment. A mathematical model, representing the 3D crane, was programmed in a Matlab script. A joystick was connected to a USB port of a computer, running the mathematical model. Fig. 9 shows the user interface (UI) with the computer program. The UI represents the top view of the 3D crane. The objective of the operators is to move the payload to the target as quickly and as accurately as possible, using the joystick. The STOP button can be pressed to stop the experiment. The $x$ and $y$ coordinates are in the $\pm 3$ m range.

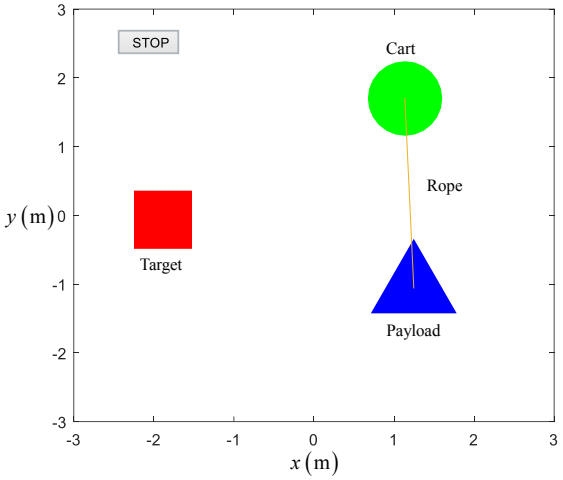


Fig. 9. User interface in the experiment.

Nonlinear governing equations of the 3D crane are given in [20] as

$$\begin{aligned}
f_x &= (M_x + m)\ddot{x} + ml\cos\theta_x\cos\theta_y\ddot{\theta}_x - ml\sin\theta_x\sin\theta_y\ddot{\theta}_y \\
&\quad + m\sin\theta_x\cos\theta_y\ddot{l} + b_x\dot{x} + 2m\cos\theta_x\cos\theta_y\dot{l}\dot{\theta}_x \\
&\quad - 2m\sin\theta_x\sin\theta_y\dot{l}\dot{\theta}_y - ml\sin\theta_x\cos\theta_y\dot{\theta}_x^2 \\
&\quad - 2ml\cos\theta_x\sin\theta_y\dot{\theta}_x\dot{\theta}_y - ml\sin\theta_x\cos\theta_y\dot{\theta}_y^2, \\
0 &= ml^2\cos^2\theta_y\ddot{\theta}_x + ml\cos\theta_x\cos\theta_y\ddot{x} + 2ml\cos^2\theta_y\dot{l}\dot{\theta}_x \\
&\quad - 2ml^2\sin\theta_y\cos\theta_y\dot{\theta}_x\dot{\theta}_y + mgl\sin\theta_x\cos\theta_y, \\
f_y &= (M_y + m)\ddot{y} + ml\cos\theta_y\ddot{\theta}_y + m\sin\theta_y\ddot{l} + b_y\dot{y} \\
&\quad + 2m\cos\theta_y\dot{l}\dot{\theta}_y - ml\sin\theta_y\dot{\theta}_y^2, \\
0 &= ml^2\ddot{\theta}_y + ml\cos\theta_y\ddot{y} - ml\sin\theta_x\sin\theta_y\ddot{x} + 2ml\dot{l}\dot{\theta}_y \\
&\quad + ml^2\cos\theta_y\sin\theta_y\dot{\theta}_x^2 + mgl\cos\theta_x\sin\theta_y,
\end{aligned} \tag{3}$$

where $f_x$ and $f_y$ are the forces applied to the cart in the $x$ and $y$ directions; $M_x$ and $M_y$ are the system moving masses in the $x$ and $y$ directions; $b_x$ and $b_y$ are the viscous damping constants for the $x$ and $y$ motions; and $m$ is the payload mass.

The nonlinear governing equations above can be linearized, and transfer functions can be obtained as

$$\begin{aligned}
\frac{\Theta_x}{F_x} &= \frac{s}{-M_x ls^3 - b_x ls^2 - g(M_x + m)s - b_x g}, \\
\frac{X}{F_x} &= \frac{(-ls^2 - g)}{-M_x ls^4 - b_x ls^3 - g(M_x + m)s^2 - b_x gs}, \\
\frac{\Theta_y}{F_y} &= \frac{s}{-M_y ls^3 - b_y ls^2 - g(M_y + m)s - b_y g}, \\
\frac{Y}{F_y} &= \frac{(-ls^2 - g)}{-M_y ls^4 - b_y ls^3 - g(M_y + m)s^2 - b_y gs}.
\end{aligned} \tag{4}$$

Using the crane parameters as those in [21], which are $l = 10\text{m}$, $m = 5\text{kg}$, $M_x = 800\text{kg}$, $b_x = 3,000\text{kg/s}$, $M_y = 500\text{kg}$, and $b_y = 2,000\ \text{kg/s}$, the natural frequencies and damping ratios in the $x$ and $y$ directions can be found from the transfer functions above as

$$\omega_{nx} = 0.991\ \text{rad/s},\ \zeta_x = 7.717\times10^{-4},$$
$$\omega_{ny} = 0.991\ \text{rad/s},\ \zeta_y = 0.0012.$$

These mode parameters were used in designing the input shapers. The transfer functions (4) were also used in designing the Smith predictor whereas the nonlinear governing equations (3) were used as the truth model, representing the 3D crane in the experiment.

An 8-point game, similar to that in physical therapy, was developed to evaluate the manual control performance of several human operators. Fig. 10 shows the UI of the designed 8-point game. The human operator must use the joystick to place the payload on the target within a specified tolerance before the target is moved to a new position. The target is moved alternately between the center point and each of the eight perimeter points. The order of the perimeter points is random. Once all the eight perimeter points are covered, the game stops, and the time to finish and the root-mean-square tracking error are recorded.

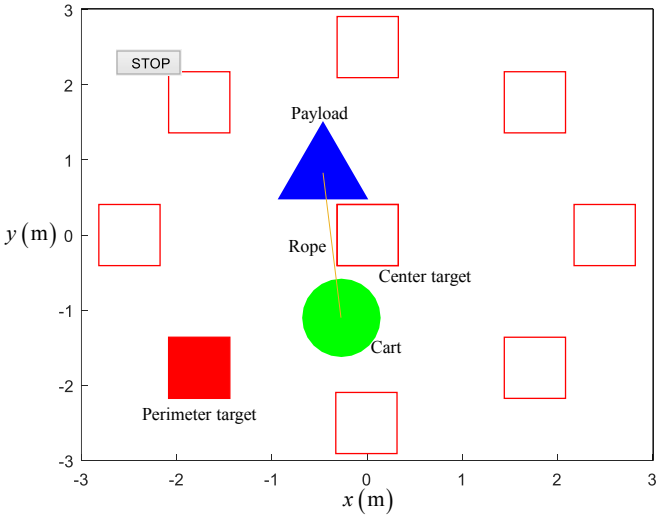


Fig. 10. User interface in the 8-point game.

Fig. 11 shows a diagram of the anti-delay CLIS, applied to the 3D crane. $C$ is the human controller with a joystick actuator. Positions of the targets were converted to references, $r_x$ and $r_y$, in the Cartesian coordinates. The ZV input shapers, $IS_x$ and $IS_y$, were used to shape the operator commands, $u_x$ and $u_y$, respectively. The Smith predictors, $SM_x$ and $SM_y$, are given by (1), where the plant models are given by (4). The actual plant, $P$, is the nonlinear plant (3), whose outputs are $x$, $y$, $\theta_x$, and $\theta_y$. The payload position is computed according to $\left(x + l\sin\theta_x,\ y + l\sin\theta_y\right)$. The sampling time used was $t_s = 0.05$ ms. The specified tolerance that must be achieved before moving on to the new target is according to the formula

$$\frac{1}{10}\int_{t-10}^{t}\sqrt{\left[r_x - \left(x + l\sin\theta_x\right)\right]^2 + \left[r_y - \left(y + l\sin\theta_y\right)\right]^2}\,dt < 0.05,$$

which is a 10 seconds moving window-average of the distance from the payload to the target.

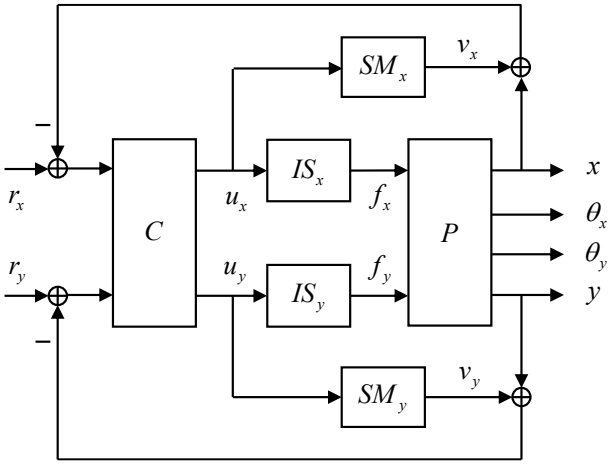


Fig. 11. Anti-delay CLIS for 3D crane.

Four cases, which were compared in the experiments, are the anti-delay CLIS with perfect plant parameters, the anti-delay CLIS with 20% uncertain plant parameters, the closed-loop signal shaping, and the without input shaper case.

Comparison criteria are a quantitative performance criteria, which is the time to complete the game and a subjective difficulty criterion based on the Cooper-Harper rating scale, presented in [10]. The rating scale is shown in Table 1.

TABLE I. SUBJECTIVE DIFFICULTY RATING SCALE (TAKEN DIRECTLY FROM [10])

| Rating | Description |
|---|---|
| 1-3 | Desired performance attainable with zero (1) to minimal (3) mental effort/compensation |
| 4-6 | Desired performance requires moderate (4) to intense (6) mental effort/compensation |
| 7-9 | Desired performance not met; Maintaining control requires mild (7) to intense (9) effort |
| 10 | Control cannot be maintained |

Fifteen persons participated in the experiments. Each of them performed all four experimental cases twice; the first round was for practice and the second round was for the record. The results are summarized in Fig. 12 and Fig. 13.

Fig. 12 shows the average time to finish the game (together with minimum, maximum, and range) for all four cases. The average was computed from fifteen persons. The proposed anti-delay CLIS used 131 seconds on average, compared to 311 seconds of the CLSS, a 57.8 percent improvement. With 20% plant parameter uncertainty, the performance of the anti-delay CLIS degraded but not substantially. This is mainly due to increasing payload swing from imperfect input shaper and Smith predictor. The anti-delay CLIS also received smallest deviation between the minimum and maximum time,

compared to the CLSS and without input shaper. This indicates that the human operator does not require special skill to track the target.

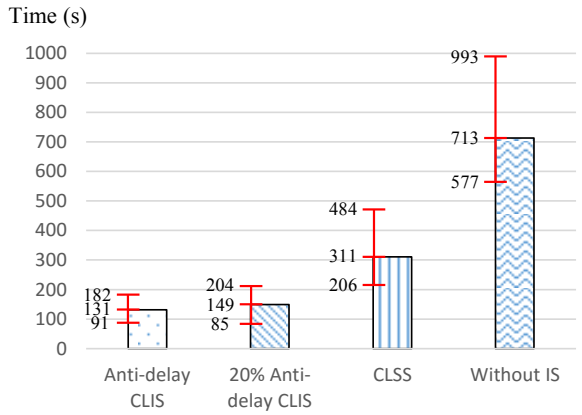


Fig. 12. Time to finish the 8-point game.

Fig. 13 shows the average subjective difficulty over fifteen persons for all four cases. The proposed anti-delay CLIS has an average subjective difficulty of 2.3, compared to 5.3 of the CLSS, a 56.6 percent improvement. Operators indicated that rather intense effort is required to complete the game using the CLSS, whereas minimal effort is required using the proposed anti-delay CLIS. The subjective difficulty slightly increases when the plant model has 20% uncertainty. Without the input shaper, two operators indicated that the control was not possible.

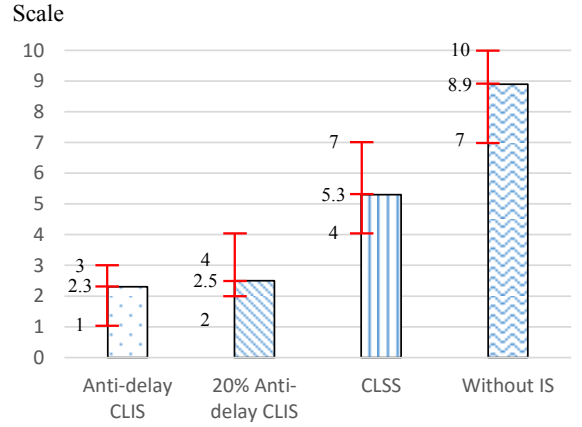


Fig. 13. Subjective difficulty.

When the input shaper was changed to the ZVD shaper, the conclusions were similar to those of the ZV shaper. This is because, using other types of shaper should affect the performance in the same way for both anti-delay CLIS and CLSS.

## V. Conclusions

Human control experiments have shown the effectiveness of the proposed anti-delay closed-loop input shaping technique. The human operators move the flexible system faster with less subjective difficulty.

Future work includes comparison between the proposed technique and other overshoot reduction techniques and implementation with actual hardware.

## References


[1] O. J. M. Smith, "Posicast control of damped oscillatory systems," *Proc. of the IRE*, vol. 45, no. 9, pp. 1249–1255, Sep. 1957.

[2] N. C. Singer and W. C. Seering, "Preshaping command inputs to reduce system vibration," *J. of Dynamic Systems, Measurement and Control*, vol. 112, no. 1, pp. 76–82, Mar. 1990.

[3] J. R. Huey and W. Singhose, "Experimental verification of stability analysis of closed-loop signal shaping controllers," in *Proc. IEEE/ASME AIM*, Monterey, CA, 2005, pp. 1587–1592.

[4] R. Tang and J. Huang, "Control of bridge cranes with distributed-mass payloads under windy conditions," *Mechanical Systems and Signal Processing*, vol. 72–73, pp. 409–419, May 2016.

[5] M. J. Maghsoudi, Z. Mohamed, A. R. Husain, and M. O. Tokhi, "An optimal performance control scheme for a 3D crane," Mechanical Systems and Signal Processing, vol. 66–67, pp. 756–768, Jan. 2016.

[6] J. J. Potter, C. J. Adams, and W. Singhose, "A planar experimental remote-controlled helicopter with a suspended load," *IEEE/ASME Transactions on Mechatronics*, vol. 20, no. 5, pp. 2496–2503, Oct. 2015.

[7] J. R. Huey and W. Singhose, "Trends in the stability properties of CLSS controllers: a root-locus analysis," *IEEE Trans. on Control Systems Tech.*, vol. 18, no. 5, pp. 1044–1056, Sep. 2010.

[8] J. R. Huey, K. L. Sorensen, and W. E. Singhose, "Useful applications of closed-loop signal shaping controllers," *Control Engineering Practice*, vol. 16, no. 7, pp. 836–846, Jul. 2008.

[9] W. Chatlatanagulchai, P. Poedaeng, and N. Pongpanich, "Improving closed-loop signal shaping of flexible systems with Smith predictor and quantitative feedback," *Engineering Journal*, vol. 20, no. 4, Oct. 2016.

[10] J. J. Potter and W. E. Singhose, "Design and human-in-the-loop testing of reduced-modification input shapers," *IEEE Transactions on Control Systems Technology*, pp. 1–8, 2015.

[11] J. J. Potter and W. E. Singhose, "Reduced-modification input shapers for manually controlled systems with flexibility," in *Proc. ACC*, Portland, OR, 2014, pp. 2815–2820.

[12] K. E. Grosser and W. E. Singhose, "Command generation for reducing perceived lag in flexible telerobotic arms," *JSME Int. Journal Series C*, vol. 43, no. 3, pp. 755–761, 2000.

[13] J. Vaughan, A. Smith, S. J. Kang, and W. Singhose, "Predictive graphical user interface elements to improve crane operator performance," *IEEE Trans. on Systems, Man, and Cybernetics-Part A: Systems and Humans*, vol. 41, no. 2, pp. 323–330, Mar. 2011.

[14] J. Vaughan, P. Jurek, and W. Singhose, "Reducing overshoot in human-operated flexible systems," *J. of Dynamic Systems, Measurement, and Control*, vol. 133, no. 1, pp. 1–10, Dec. 2010.

[15] C. F. Cutforth and L. Y. Pao, "Control using equal length shaped commands to reduce vibration," *IEEE Trans. on Control Systems Tech.*, vol. 11, no. 1, pp. 62–72, Jan. 2003.

[16] R. A. Masterson, W. E. Singhose, and W. P. Seering, "Setpoint generation for constant-velocity motion of space-based scanners," *J. of Guidance, Control, and Dynamics*, vol. 23, no. 5, pp. 892–895, Sep. 2000.

[17] J. J. Potter and W. Singhose, "Improving manual tracking of systems with oscillatory dynamics," *IEEE Transactions on Human-Machine Systems*, vol. 43, no. 1, pp. 46–52, Jan. 2013.

[18] J. J. Potter and W. Singhose, "Using manual tracking performance to tune a specified-negative-amplitude input shaper," in *Proc. IEEE SMC*, Seoul, Korea, 2012, pp. 1503–1508.

[19] W. Chatlatanagulchai and P. Poedaeng, "Closed-loop input shaping with Smith predictor and quantitative feedback control," in *Proc. MENETT*, Nakhon Ratchasima, Thailand, 2015, pp. 846–853.

[20] H.-H. Lee, "Modeling and control of a three-dimensional overhead crane," *J. of Dynamic Systems, Measurement, and Control*, vol. 120, no. 4, pp. 471–476, Dec. 1998.

[21] J. Stergiopoulos and A. Tzes, "An adaptive input shaping technique for the suppression of payload swing in three-dimensional overhead cranes with hoisting mechanism," in *Proc. ETFA*, Patras, Greece, 2007, pp. 565–568.